Atmospheric
Chemistry
and Physics

Toward enhanced capability for detecting and predicting dust events in the western United States: the Arizona case study

M. Huang[1,2], **D. Tong**[1,2,3], **P. Lee**[1], **L. Pan**[1,3], **Y. Tang**[1,3], **I. Stajner**[4], **R. B. Pierce**[5], **J. McQueen**[6], **and J. Wang**[1]

[1]NOAA/OAR/ARL, NOAA Center for Weather and Climate Prediction, College Park, MD 20740, USA
[2]Center for Spatial Information Science and Systems, George Mason University, Fairfax, VA 22030, USA
[3]Cooperative Institute for Climate and Satellites, University of Maryland, College Park, MD 20740, USA
[4]NOAA/NWS/STI, Silver Spring, MD 20910, USA
[5]NOAA/NESDIS, Madison, WI 53706, USA
[6]NOAA/NWS/NCEP/EMC, NOAA Center for Weather and Climate Prediction, College Park, MD 20740, USA

Correspondence to: M. Huang (mhuang10@gmu.edu)

Abstract. Dust aerosols affect human life, ecosystems, atmospheric chemistry and climate in various aspects. Some studies have revealed intensified dust activity in the western US during the past decades despite the weaker dust activity in non-US regions. It is important to extend the historical dust records, to better understand their temporal changes, and to use such information to improve the daily dust forecasting skill as well as the projection of future dust activity under the changing climate. This study develops dust records in Arizona in 2005–2013 using multiple observation data sets, including in situ measurements at the surface Air Quality System (AQS) and Interagency Monitoring of Protected Visual Environments (IMPROVE) sites, and level 2 deep blue aerosol product by the Moderate Resolution Imaging Spectroradiometer. The diurnal and inter-annual variability of identified dust events are shown related to observed weather patterns (e.g., wind and soil moisture) and surface conditions (e.g., land cover type and vegetation conditions), suggesting a potential for use of satellite soil moisture and land products to help interpret and predict dust activity. Backtrajectories computed using NOAA's Hybrid Single Particle Lagrangian Integrated Trajectory (HYSPLIT) model indicate that the Sonoran and Chihuahuan deserts are important dust source regions during identified dust events in Phoenix, Arizona. Finally, we assess the impact of a recent strong dust event on western US air quality, using various observational and modeling data sets, during a period with a stratospheric ozone intrusion event. The capability of the current US National Air Quality Forecasting Capability (NAQFC) Community Multi-scale Air Quality (CMAQ) modeling system to represent the magnitude and the temporal variability of aerosol concentrations is evaluated for this event. Directions for integrating observations to further improve dust emission modeling in CMAQ are also suggested.

1 Introduction

Dust aerosols, generated by anthropogenic or natural sources, present strong spatial and temporal variability (Ginoux et al., 2001, 2010, 2012a, b; Carslaw et al., 2010; Prospero et al., 2002; Zender et al., 2004) and affect human life, ecosystems, atmospheric chemistry and climate in many aspects. Degraded visibility during dusty periods prevents normal outdoor activities and transportation, and dust activity may be associated with a number of human diseases such as "valley fever", "haboob lung syndrome" and certain eye diseases (Sprigg et al., 2014; Goudie, 2013; Panikkath et al., 2013; Liu et al., 2009a; Morain et al., 2010). Dust neutralizes acid rain (Hedin and Likens, 1996) and interacts with terrestrial and ocean ecosystems (Gassó et al., 2010; Chen et al., 2013; Yu et al., 2015; Reynolds et al., 2001, 2006). Also, dust absorbs sunlight, reduces the planetary albedo over bright surfaces such as snow, ice and deserts, and modifies cloud properties and precipitation (Zhao et al., 2012; Creamean et al., 2013, 2015). The deposition of dust on snow and ice

can accelerate their melting and affect regional climate (e.g., Carslaw et al., 2010; Painter et al., 2007). In addition, mineral dust aerosols affect atmospheric chemistry through surface adsorption and reactions (Dentener et al., 1996; Grassian, 2001; Underwood et al., 2001; Fairlie et al., 2010).

North America contributes to a small proportion of the world's total dust emissions, ranging from < 0.1 to ∼ 5 % as reported in previous studies (Miller et al., 2004a, b; Tanaka and Chiba, 2006; Zender et al., 2003; Ginoux et al., 2004; Ravi et al., 2011), and the important emitters include the four major deserts in the western US, i.e., the Great Basin, Mojave, Sonoran, and Chihuahuan deserts. Dust storms in the western US usually last for 2–21 h, due to various mechanisms (Lei and Wang, 2014). Surface and satellite observations, along with modeling analysis, have provided evidence that the western US is not only affected by local dust emissions but is also susceptible to dust transported from overseas (e.g., Van Curen and Cahill, 2002; Fischer et al., 2009; Uno et al., 2009; Fairlie et al., 2007; Chin et al., 2007; Eguchi et al., 2009; Stith et al., 2009; Dunlea et al., 2009; Liu et al., 2009b). Using a global transport model, Fairlie et al. (2007) reported that dust from overseas contributed to < 30 % of the total dust in the southwestern US, to > 80 % of the total dust in the northwestern US in spring 2001, and that these non-US contributions were much larger than in other seasons. Recent dust observations have revealed rapid intensification of dust storm activity in the western US (e.g., Brahney et al., 2013), despite the weaker dust activity in many non-US regions (e.g., Mahowald et al., 2007; Zhu et al., 2008; Shao et al., 2013). This increasing trend enhances the concerns about their various impacts and even the possibility of another Dust Bowl, as that which occurred in the 1930s due to severe drought conditions and inappropriate farming methods (Lee and Gill, 2015; http://www.livinghistoryfarm.org/farminginthe30s/water_02.html; http://www.ncdc.noaa.gov/paleo/drought/drght_history.html) and led to significantly negative agricultural and ecological impacts in the western/central US.

Surface and satellite observations have been used to study dust trends and variability, as well as for model evaluation (e.g., Tong et al., 2012; Appel et al., 2013; Torres et al., 2002; Ginoux and Torres, 2003; Draxler et al., 2010; Vukovic et al., 2014; Mahler et al., 2006; Raman and Arellano, 2013; Morain et al., 2010). Surface observations used in many of these studies are sparsely and/or infrequently sampled, and there is delay for obtaining some of these data sets which prevents timely updates on the observed dust records. The capability of satellite aerosol optical depth products to capture the dust events depends on various factors such as sensor characteristics, cloud conditions, surface reflectance and dust mineralogy (e.g., Baddock et al., 2009). There is still a lack of comprehensively developed observational dust records with broad spatial coverage up to the very recent years, and accurately simulating dust aerosols is challenging. Therefore, it is important to extend the temporal changes of observed dust activity to recent years using diverse observations. These various observations can assist in evaluating the chemical transport model skills especially during dust events. Furthermore, better understanding the linkages between the temporal changes of dust observations and the observed surface/weather conditions can be beneficial for advancing the dust emission modeling skills via improving the meteorology and dust source input data, as well as for projecting future dust activity under the changing climate.

Several studies found that dust events can be accompanied by stratospheric intrusions in multiple regions of the world (e.g., Pan and Randel, 2006; Yasunari et al., 2007; Yasunari and Yamazaki, 2009; Reddy and Pierce, 2012). Recently, substantial attention has been called on the influences of stratospheric ozone intrusions on western US surface/near-surface ozone variability (e.g., Lin et al., 2012; Langford et al., 2014). Observations and modeling tools are useful for identifying the periods when dust events are associated with stratospheric intrusions, as well as to assess the impact of elevated surface/near-surface ozone and PM (particulate matter) concentrations on public health and the environment during such events.

This study develops decadal dust records in the state of Arizona using multiple in situ and satellite observation data sets, and relates the diurnal and inter-annual variability of observed dust activity to the observed surface conditions (e.g., land cover type and vegetation conditions) and weather patterns (e.g., wind and soil moisture; Sects. 3.1–3.3). We also analyze observations and model simulations during a recent strong dust event in the western US accompanied by a stratospheric ozone intrusion. The modeling analyses include the US National Air Quality Forecasting Capability (NAQFC) 12 km Community Multi-scale Air Quality (CMAQ) regional model base and sensitivity simulations (Sect. 3.4). In the analyses, we discuss the usefulness and limitations of different observations for identifying potential exceptional events and for model evaluation. We also suggest future directions of integrating observations into regional dust emission modeling in the western US for further improvement of the air quality forecasts.

2 Data and method

2.1 Drought indicators

Three data sets were analyzed to interpret the observed inter-annual variability of the drought conditions from 2005 to 2013 in Arizona, an important dust source and receptor region in the western US. They are the normalized difference vegetation index (NDVI) from the Moderate Resolution Imaging Spectroradiometer (MODIS) instrument on the NASA Aqua satellite, a European soil moisture data set that merged both passive and active satellite sensor data, and the Palmer drought severity index (PDSI).

Table 1. Data used in this study*.

Data type	Sensor or network	Variable	Temporal resolution	Mainly focused-on location(s)	Data source or reference
Surface conditions/ drought indicators (Sects. 2.1–2.2)	Aqua MODIS	satellite NDVI	monthly	AZ	https://lpdaac.usgs.gov/dataset_discovery/modis/
	ESA/CCI	satellite soil moisture	daily	AZ	http://www.esa-soilmoisture-cci.org/
	PDSI	drought index	monthly	southwestern AZ	http://www.ncdc.noaa.gov/temp-and-precip/drought
	Terra & Aqua MODIS	satellite land cover type	yearly	western US	https://lpdaac.usgs.gov/dataset_discovery/modis/
Aerosol observations (Sect. 2.3)	Terra & Aqua MODIS	satellite AOD (deep blue algorithm)	by swath, ~ twice/day in the late morning and early afternoon	AZ	http://ladsweb.nascom.nasa.gov/data/
	IMPROVE	in situ PM	24 h average, every 3 days	Phoenix, AZ	http://views.cira.colostate.edu/fed/DataWizard/Default.aspx
	AQS & AirNow	in situ PM	hourly	Phoenix, AZ	http://www.epa.gov/ttn/airs/airsaqs/detaildata/downloadaqsdata.htm; www.epa.gov/airnow/2013
	NOAA HMS	satellite dust and smoke detection	updated ~ twice/day	western US	http://www.ssd.noaa.gov/PS/FIRE/smoke.html
	Aqua AIRS	satellite daytime dust score	daily	western US	https://earthdata.nasa.gov/labs/worldview/
Meteorological observations (Sect. 2.4)	AZMET	in situ wind	hourly	Phoenix, AZ	http://ag.arizona.edu/azmet/index.html
	HYSPLIT w/ NARR meteorology	trajectory endpoints	hourly	western US	http://ready.arl.noaa.gov/HYSPLIT.php
Models (Sect. 2.5, 2.6)	NAM (12 km)	meteorology	hourly (for NAQFC)	western US	http://www.emc.ncep.noaa.gov/mmb/mmbpll/opsnam/
	FENGSHA	dust emissions	hourly	western US	Tong et al. (2015)
	GEOS-Chem ($4° \times 5°$)	various species	monthly (2006)	global	http://www.geos-chem.org/; http://acmg.seas.harvard.edu/geos/geos_chem_narrative.html; Barrett et al. (2012)
	NAQFC CMAQ (12 km)	PM2.5	hourly	western US	Chai et al. (2013); Pan et al. (2014)
	RAQMS ($1°$)	daytime ozone, relative humidity	6 hourly	western US	http://raqms-ops.ssec.wisc.edu/
(Sects. 2.3, 2.7)	AQS	in situ NO_x and CO	hourly	Phoenix, AZ	http://www.epa.gov/ttn/airs/airsaqs/detaildata/downloadaqsdata.htm
	Aqua AIRS	daytime ozone and CO profiles	daily	western US	http://disc.sci.gsfc.nasa.gov/

* Abbreviations in alphabetical order: AIRS: Atmospheric Infrared Sounder, AOD: aerosol optical depth, AQS: Air Quality System, AZ: Arizona, AZMET: Arizona Meteorological Network, CMAQ: Community Multi-scale Air Quality, CO: carbon monoxide, ESA/CCI: European Space Agency/Climate Change Initiative, HMS: Hazard Mapping System, HYSPLIT: Hybrid Single Particle Lagrangian Integrated Trajectory, IMPROVE: Interagency Monitoring of Protected Visual Environments, MODIS: Moderate Resolution Imaging Spectroradiometer, NAM: North American Mesoscale Forecast System, NARR: North America Regional Reanalysis, NAQFC: National Air Quality Forecasting Capability, NDVI: normalized difference vegetation index, NOAA: National Oceanic and Atmospheric Administration, NO_x: oxides of nitrogen, PDSI: Palmer drought severity index, PM: particulate matter, RAQMS: Realtime Air Quality Modeling System.

NDVI is the most commonly used vegetation index, calculated using the reflected visible and near-infrared light by vegetation (Scheftic et al., 2014; Brown et al., 2006). Smaller NDVI values refer to less vegetated areas, which may have a high potential of emitting dust (D. Kim et al., 2013; Vukovic et al., 2014). NDVI has been used for monitoring land cover changes and indicating drought (Tucker and Choudhury, 1987; Karnieli et al., 2010; Wan et al., 2004), and it has been found to be correlated with meteorologically based drought indexes such as the standardized precipitation index (Ji and Peters, 2003). In this study we used the monthly mean 1 km MODIS NDVI product Collection 5, which temporally aggregated the 16-day 1 km MODIS NDVI using a weighted average. Following the users' guide instructions (http://vip.arizona.edu/documents/MODIS/MODIS_VI_UsersGuide_01_2012.pdf), only the data flagged as good quality were used. To avoid the known effects from the degradation of the Terra MODIS sensor (e.g., Wang et al., 2012), only the NDVI data from the Aqua MODIS (MYD13A3) were used.

Soil moisture has also been used for drought monitoring and several studies have found that satellite and modeled soil moisture is related to dust outbreaks in Asian countries (Liu et al., 2004; Y. Kim et al., 2013; Kim and Choi, 2015). This study used a multi-sensor satellite soil moisture product from the European Space Agency (ESA) within the soil moisture Climate Change Initiative (CCI) project that merged all available passive and active products and preserved the original dynamics of these remote sensing observations. The data are produced daily on a $0.25° \times 0.25°$ horizontal resolution grid. Long-term soil moisture changes in the US based on the CCI soil moisture product contributed to the US National Climate

Assessment report (Melillo et al., 2014, pp.72–73, last accessed November 2015).

Monthly PDSI data, calculated from temperature and precipitation (Palmer, 1965; Alley, 1984), are widely used for identifying long-term and abnormal moisture deficiency or excess. Studies have found that PDSI is moderately or significantly correlated ($r = 0.5$ to 0.7) with observed soil moisture content within the top 1 m depth during warm-season months in various regions (Dai et al., 2004). In this study, we analyzed the inter-annual variability of PDSI in two NOAA climate regions in Arizona (Karl and Koss, 1984; http://www.ncdc.noaa.gov/monitoring-references/maps/us-climate-regions.php). Drought conditions are defined with negative PDSI values (e.g., -2 is moderate drought, -3 is severe drought, and -4 is extreme drought), and positive PDSI values indicate wet conditions.

2.2 Specification of dust sources using satellite (MODIS) land cover and NDVI products

The dust productive areas depend on surface conditions such as land cover types and vegetation conditions, and therefore are temporally variable. Several studies specified dynamic dust source regions using either or both satellite land cover types and NDVI products (e.g., Vukovic et al., 2014; Yin et al., 2007; D. Kim et al., 2013). In this study, to explore the inter-annual variability of dust sources in the western US and its influences on the dust activity, we specified the dust sources following the methods in Vukovic et al. (2014). First, for each year during 2005–2013, we located open shrubland, cropland, and barren areas where dust can potentially be emitted from, accord-

ing to the annual-mean MODIS land cover type product Collection 5.1 (MCD12Q1, 500 m resolution in tile grid; Friedl et al., 2010) and its 17-category International Geosphere Biosphere Programme (IGBP) land cover classification scheme (defined at: https://lpdaac.usgs.gov/dataset_discovery/modis/modis_products_table/mcd12q1). Then, for each month and each of the three erodible land cover types, dust source areas were determined based on the monthly mean Aqua MODIS NDVI values (introduced in Sect. 2.1) and the following criteria.

– Barren (category 16): 100 % dust source (independent from NDVI).

– Cropland and cropland/native vegetation (categories 12 and 14): if NDVI $\leq$ 0.25, 100 % dust source.

– Open shrubland (category 7): if NDVI $\leq$ 0.1, 100 % dust source; if NDVI is within 0.11–0.13, decreasing linearly from 70 to 30 % as a dust source.

2.3 Aerosol observations

Both remote sensing and in situ aerosol observations were used to explore the dust aerosol distributions in Arizona. We first demonstrate the large-scale spatial distributions of aerosols using satellite aerosol products and discuss their diurnal (e.g., late morning vs. early afternoon times) and interannual variability link to the weather and surface conditions. We mainly focus on spring and summer time periods when dust activity is generally strong in Arizona, as found by Ginoux et al. (2012a) for the 2003–2009 period. In situ observations at Arizona surface monitoring sites were then analyzed, focusing on their temporal variability in the populated Phoenix urban area (i.e., with a population of $\sim$ 1.5 million). Finally, we identify dust events in Phoenix using hourly surface observations and discuss the time of occurrence of these identified dust events.

2.3.1 MODIS deep blue aerosol optical depth (AOD) and dust optical depth (DOD)

We extracted scenes dominated by dust aerosols from the MODIS level 2 deep blue aerosol product Collection 6 (Hsu et al., 2013) during 2005–2013. This product includes the values of AOD and single scattering albedo (SSA) at 412, 470, 550, and 670 nm, as well as the Ångström exponent between 412 and 470 nm. It is recommended for identifying both dust sources and plumes at high spatial resolution (e.g., Baddock et al., 2009). The Collection 6 deep blue data were created using the enhanced deep blue algorithm (from the previous Collection 5.1), with improved surface reflectance determination, aerosol model selection, and cloud screening schemes. Also, the deep blue data from Terra MODIS have been extended beyond 2007 using suitable calibration corrections (Hsu et al., 2013). Compared with the Aerosol Robotic Network (AERONET) AOD data, the Collection 6 deep blue AOD data from Aqua MODIS show a $\sim$ 0.03 change in bias

through the decade, with overall negative biases in 2005–2007 and 2011, and positive biases in 2009, 2010, and 2012 (Sayer et al., 2013).

The very good (quality assurance flag = 3, as recommended by Shi et al., 2013, and Sayer et al., 2013) MODIS deep blue AOD data from Terra and Aqua were selected and gridded on $0.1° \times 0.1°$ horizontal resolution for each day. The DOD values were then determined by screening the 550 nm AOD data based on three criteria to represent dust-dominated scenes: (1) an Ångström exponent within 0–0.5, which selects the particles in large sizes; (2) SSA at 412 nm, < 0.95, which selects the absorbing aerosols and efficiently eliminates the sea-salt-dominated scenes; and (3) a positive difference of SSA between 412 and 670 nm, due to the specific optical property of dust by which there is a sharp increase of absorption from red to deep blue (Ginoux et al., 2012a; Hsu et al., 2013).

2.3.2 Particulate matter (PM) measurements from the surface Interagency Monitoring of Protected Visual Environments (IMPROVE) sites

Most IMPROVE surface sites are located in rural regions, many of which are in the national parks to measure background pollution levels. Here, we analyzed the temporal variability of observed particulate matter mass PM10 (i.e., < 10 μm in diameter) along with the fine (i.e., < 2.5 μm in diameter) soil particles at the Phoenix site (PHOE1, 33.5038° N, 112.0958° W) within the IMPROVE network during 2005–2013. These fine soil data are computed based on five (Al, Si, Ca, Fe, and Ti) soil-derived trace metals in their assumed oxidized form measured at the IMPROVE site (Malm et al., 2004). Daily mean IMPROVE data are available every 3 days, and there is an approximate delay of 1 year for obtaining these data.

2.3.3 Air Quality System (AQS) and AirNow PM and trace gas measurements

In general the US Environmental Protection Agency (EPA) AQS sites are designed to monitor air quality in populated urban or suburban areas. In this study the AQS hourly PM10 and PM2.5 data from 2005 to September 2013 and the AirNow from September to December 2013 at the Phoenix JLG supersite (co-located with the IMPROVE PHOE1 site, AQS site no. 040139997) were analyzed to study the temporal variability of dust events on hourly temporal resolution. In the case study on the dusty year of December 2006–November 2007, AQS trace gas measurements (i.e., carbon monoxide, CO, and oxides of nitrogen, NO_x) were used as tracers of anthropogenic or biomass burning sources to evaluate the dust events that are identified based on the hourly PM observations. The AQS data qualifier codes were also examined, which provided us with clues of the event types

(e.g., high winds and long-range transport of PM from non-US regions).

2.3.4 Other satellite aerosol products

The achieved NOAA Hazard Mapping System (HMS) text product narratively describes the observed smoke and dust events based on images of multiple satellites. It qualitatively indicates the dust's locations and the intensity, which in this study supports the analysis during a recent strong event we selected for the case study in Sect. 3.4. We also used the dust score data from the Atmospheric Infrared Sensor (AIRS) instrument on board the Aqua satellite to qualitatively represent the presence of atmospheric dust during this recent event. The Aqua satellite has ascending overpass times in the early afternoon ($\sim$ 13:30 LT, local time).

2.4 Observed wind speed and direction

As atmospheric dust concentrations depend on the wind fields (e.g., Kavouras et al., 2007; Ravi et al., 2011; Csavina et al., 2014), we used the observed hourly surface wind speed and direction in December 2006–November 2007 at the Phoenix Encanto site (33.4792° N, 112.0964° W, within the Arizona meteorological network; AZMET) together with the hourly AQS PM observations to identify the dust events. Phoenix Encanto is the closest site to the Phoenix JLG supersite within the AZMET that had meteorological observations available during this period.

2.5 Backward air mass trajectory analysis

Backward air mass trajectories were computed to locate the sources of dust aerosols observed at the Phoenix JLG site during the identified dust events in December 2006–November 2007. These trajectories were calculated using NOAA's Hybrid Single Particle Lagrangian Integrated Trajectory (HYSPLIT) model, version 4 (Draxler and Rolph, 2015; Stein et al., 2015). The accuracy of the trajectories depends on the resolution of the wind data (Draxler and Hess, 1998), and we calculated these trajectories based on the 3-hourly North America Regional Reanalysis (NARR) data (Mesinger et al., 2006) on 32 km horizontal resolution and nine vertical levels below 800 hPa. NARR is the finest meteorology HYSPLIT can currently run with for studying this year, as the horizontally finer (12 km) North American Mesoscale Forecast System (NAM; Janjic, 2003; Janjic et al., 2004) wind fields are only available for HYSPLIT calculations for the time after May 2007. These trajectories were initiated at 500 m above Phoenix's ground level at identified dust periods and were computed for 24 h. The HYSPLIT-indicated air mass origins during the Phoenix dust events will be discussed together with the MODIS land cover product (details in Sect. 2.2).
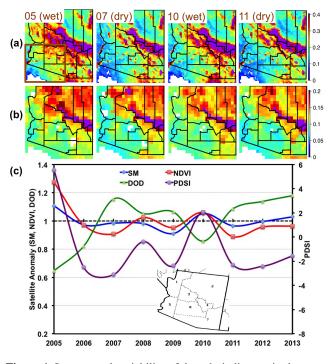

Figure 1. Inter-annual variability of drought indicators in dust seasons: (a) MODIS NDVI on 0.1° × 0.1° horizontal resolution and (b) ESA multi-sensor soil moisture (SM) product on 0.25° × 0.25° resolution are shown on selected moderate-to-severe dry and wet years. The text in the upper left corner of each panel indicates the year of the data. (c) Time series of PDSI and the anomalies (i.e., the annual mean value over the multi-year mean value) of satellite SM, NDVI and Aqua MODIS DOD. The anomalies of satellite data were calculated using data within the box defined in (a). The inset panel in (c) shows the NOAA climate divisions, and PDSI values in the southwest (region 5) and south central (region 6) regions were used in the time series plot.

2.6 Chemical transport model base and sensitivity simulations

The US NAQFC 12 km CMAQ (Byun and Schere, 2006; Chai et al., 2013; Pan et al., 2014) model simulations were used to depict the PM distributions during a recent strong dust event in the western US that was accompanied by a stratospheric ozone intrusion. Dust emissions for NAQFC's CMAQ simulations were calculated by the FENGSHA dust emission model based on a modified Owen's equation, which is a function of wind speed, soil moisture, soil texture and erodible land use types (Tong et al., 2015). Both the FENGSHA and CMAQ model calculations were driven by meteorological fields from the NAM model, which is known to usually have positive biases in temperature, moisture, and wind speed in the continental US (e.g., McQueen et al., 2015a, b). The CMAQ base simulation was evaluated against surface observations at the AirNow and IMPROVE sites, and we focused on PM2.5 concentrations as it is one of the standard NAQFC products. To quantify the impact of west-
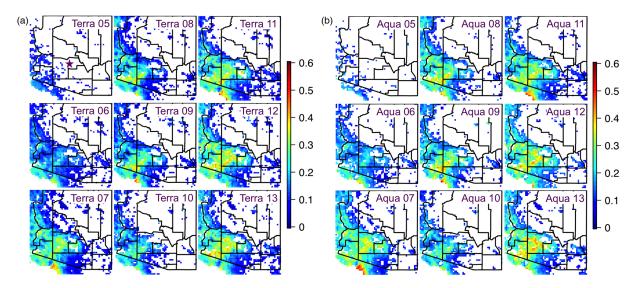
Figure 2. (a) DOD maps (in $0.1° \times 0.1°$ horizontal resolution) in dust seasons from Terra MODIS during 2005–2013. Data are plotted only for the grids in which DOD data are available > 5 % of the total number of days in each year (defined as "areas of dust impact"). The purple star in the upper left panel of **(a)** indicates the location of Phoenix. **(b)** Same as **(a)**, but for Aqua MODIS.

ern US dust emissions on PM2.5 concentrations during this event, an additional sensitivity simulation was conducted in which no dust emissions were included. NAQFC CMAQ lateral chemical boundary conditions were downscaled from a monthly mean output from a global GEOS-Chem simulation of year 2006 (http://www.geos-chem.org/; http://acmg.seas. harvard.edu/geos/geos_chem_narrative.html, and the references therein. The details of this GEOS-Chem simulation and the boundary condition downscaling methods are included in Barrett et al., 2012). These boundary conditions do not represent the day-to-day variability in the transboundary chemical species impacting the CMAQ model domain. Stratospheric ozone intrusion during this dust event is indicated by meteorological conditions and chemical fields from the global $1° \times 1°$ Realtime Air Quality Modeling System (RAQMS; Pierce et al., 2007) which assimilated satellite ozone observations.

2.7 Ozone and carbon monoxide products from AIRS

The level 3 daytime ozone and carbon monoxide (CO) profiles (AIRX3STD version 6, gridded in $1° \times 1°$ horizontal resolution) from the AIRS instrument were used to help identify the stratospheric intrusion during a recent dust event in Sect. 3.4. AIRS ozone is sensitive to the altitudes near the tropopause, with positive biases over ozonesondes in the upper troposphere (e.g., Bian et al., 2007). Due to its broad spatial coverage and the capability of reproducing the dynamical variability of ozone near the tropopause, AIRS ozone has been used in a number of studies on stratospheric intrusions (e.g., Lin et al., 2012; Pan and Randel, 2006; Pan et al., 2007). AIRS CO, which is most sensitive to 300–600 hPa (Warner et al., 2007), can distinguish stratospheric intrusions

from long-range transported pollution when used together with its ozone product.

3 Results and discussions

3.1 Decadal drought indicators, dust sources and satellite DOD in Arizona

We first review the spatial and inter-annual variability of the drought conditions during 2005–2013 in Arizona, in the dusty seasons (i.e., spring and summer, from March to August), based on satellite NDVI (Fig. 1a) and soil moisture (Fig. 1b) products. These observations show that southwestern and south central Arizona, a region close to the Sonoran Desert, is overall drier, with less greenness, than the rest of the state. Most of these dry regions fall into two NOAA climate divisions (i.e., south central including the Maricopa and Pinal counties and southwest including the La Paz and Yuma counties). The mean PDSI values in spring and summer in these two climate divisions were calculated (Fig. 1c), indicating moderate to severe dry conditions under warm weather in these regions in the past decade, except for 2005 (extremely wet), 2008 (near neutral), and 2010 (moderately wet). The PDSI values were then correlated with the anomalies of satellite NDVI and soil moisture, defined as the ratio of the annual mean value over the multi-year mean value. In general, Fig. 1c shows that the PDSI-indicated drought conditions are consistent with those based on the satellite NDVI and soil moisture products: i.e., with correlation coefficients (r) of PDSI vs. NDVI anomaly and PDSI vs. soil moisture anomaly of 0.96 and 0.84, respectively.
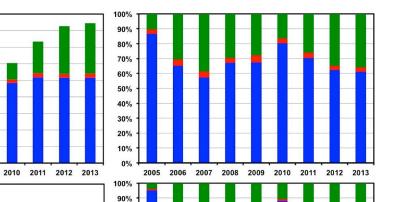
Figure 3. MODIS-derived dust sources over the western US (from the MODIS tile grid horizontal 8/vertical 5, defined in Fig. S1) and in the southwestern US (lower, defined as the region within the box in Fig. 1a), during the dust seasons in 2005–2013. The absolute source areas for three types of land cover are shown in the left column, and the contributions (%) from individual land cover types to the total source areas are shown in the right column.
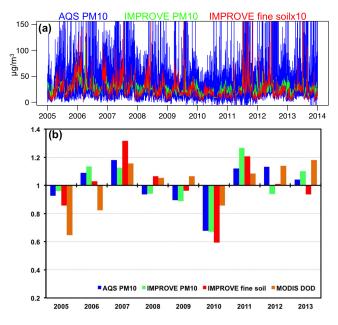

Figure 4. Time series of surface PM data at AQS and IMPROVE sites in Phoenix. These observations are shown in their original temporal resolution in (**a**), and their anomalies in each year's dust season are shown in (**b**), along with the Aqua MODIS DOD anomalies (i.e., the annual mean value over the multi-year mean value).

Gridded MODIS DOD maps are shown in Fig. 2a, b for each year's dusty season during 2005–2013 and they were related to the satellite-based weather and vegetation conditions (Fig. 1c). To exclude the locations occasionally affected by long-range transported dust aerosols, data are shown only for the grids in which DOD data are available on > 5 % of the total number of days in each year, defined as "areas of dust impact". In all maps, high DOD values (> 0.2) are seen in the dry southwest and south central climate divisions. Aqua MODIS observed higher DOD than in Terra MODIS DOD by 4–19 % (∼ 11 % on average). Assuming Terra and Aqua MODIS DOD have similar quality in this region, this indicates higher dust in the early afternoon than in the late morning. Inter-annual variability is also seen from these DOD maps over large spatial scales, with smaller "areas of dust impact" and DOD values in these areas in the wetter years (e.g., 2005 and 2010). The differences among the annual-mean DOD values are often much larger than those of the MODIS AOD biases reported by Sayer et al. (2013). The correlation coefficients between the anomalies of Aqua MODIS DOD and the three drought indicators (NDVI, soil moisture, and PDSI) in the past decade are −0.82, −0.58, and −0.79, respectively. The anomalies of Terra DOD show similar correlations with these three drought indicators. Such anticorrelations suggest the importance of drought monitoring to the interpretation and prediction of dust activity. In particular, it is noted that satellites can provide soil moisture measure-

ments of much broader spatial coverage than the surface sites (e.g., there is only one site, Walnut Gulch, in Arizona within the Soil Climate Analysis Network), and drought monitoring can be better assisted by newer satellite soil moisture observations, such as those from NASA's newly launched Soil Moisture Active Passive (SMAP).

The correlations between dust activity and drought conditions can be partially attributed to the dependency of dust source regions as well as the threshold wind velocity (i.e., the minimum wind velocity required to initiate soil erosion; Ravi et al., 2011, and the references therein) on the surface conditions in the western US. Figure 3 shows the MODIS-derived annual-mean dust source regions during the dusty season in 2005–2013 over several land use types (maps of the dust sources from three land use types are shown for selected wet and dry years in Fig. S1 in the Supplement). In most years, barren contributed the most ($> 50\%$) and cropland contributed the least ($< 5\%$) to the dust source regions, qualitatively consistent with the findings by Ginoux et al. (2012a) and Nordstrom and Hotta (2004). In general, larger dust source regions are found in drier years, with the strongest inter-annual variability from the open shrubland category. As an important nonerodible roughness element, the variable vegetation also modified the threshold wind velocity for the soil erosion. These findings suggest that dust emission modeling can be improved by using satellite land products, instead of those based on static land data. Similar land products of smaller footprints from newer satellite instruments, such as those from the Visible Infrared Imaging Radiometer Suite (VIIRS) instrument launched in 2011, can also be considered. In addition, soil moisture affects dust activity by modifying the threshold wind velocity, dependent on the soil type. Therefore, dust emission modeling can also benefit from careful evaluation and improvement of the soil moisture inputs using surface and satellite soil moisture measurements.

3.2 Decadal surface in situ PM measurements in Phoenix

We then analyze the long-term surface PM measurements at the AQS and IMPROVE monitoring sites in the Phoenix area. The time series of PM10 from AQS/AirNow and IMPROVE sites in Phoenix are shown in Fig. 4a during 2005–2013 in their original temporal resolution. It is shown that the 24 h mean IMPROVE PM10 data missed the extreme values (e.g., $> 150\,\mu\mathrm{g\,m^{-3}}$) that were captured by the hourly AQS/AirNow observations at this location. The 9-year mean PM10 concentration at the AQS site ($31.6\,\mu\mathrm{g\,m^{-3}}$) is slightly higher than at the IMPROVE site ($28.2\,\mu\mathrm{g\,m^{-3}}$) due to the different sampling frequency and methods. Another advantage of AQS/AirNow observations over those at the IMPROVE sites is that they are timely made available. IMPROVE fine soil particles demonstrate the similar temporal variability to IMPROVE PM10 with a correlation coefficient

of ~ 0.8. To explore the inter-annual variability of PM10 in dust seasons (spring–summer) at this site, we calculated the anomalies for each variable in each year (Fig. 4b). Similar to the results from satellite observations, the inter-annual variability of surface PM observations are anticorrelated with regional soil wetness and vegetation cover. Inconsistency exists among the anomalies of these three variables, due to different sampling methods and densities and because the particle size distributions depend on soil wetness (Li and Zhang, 2014). Due to the different observation methods, uncertainties, and sampling strategies (spatial and temporal), the anomalies of surface PM concentrations are more consistent with (i.e., whether > 1 or < 1) those of the MODIS DOD only in several significantly wet or dry years (i.e., 2005, 2007, 2010, 2011).

3.3 Phoenix dust events in 2007 identified by hourly surface observations

We take the dry and dusty year of December 2006–November 2007 (Fig. 4b) as an example to introduce a novel approach of identifying dust events using hourly observations. We first calculated the seasonal averages of PM10 and wind speed in Phoenix based on the AQS PM10 and AZMET wind speed observations. It is shown that in this year dominant westerly and easterly winds in spring and summer carried much PM10 to Phoenix (Fig. S2), whereas most PM10 in autumn and winter came from the north and east. Hourly mean wind speed is highly correlated with the hourly maximum wind speed ($r = 0.93$, slope $= \sim 0.5$), and stronger winds were observed during spring and summer (Fig. S3). Two steps followed to identify the individual dust events. In the first step, any period in which PM10 and wind speed exceeded the seasonal mean values for no shorter than 2 h (the lower end of dust storm duration in the western US reported by Lei and Wang, 2014) was defined as a dusty period. The second step screened the dust events selected in the first step using their median values of PM10 ($55\,\mu\mathrm{g\,m^{-3}}$) and PM2.5 / PM10 ($\sim 0.2$) as lower and upper thresholds and therefore relied on data availability of both PM2.5 and PM10. After these two steps of selection, 29 high dust periods are found as denoted in Fig. S4 on 7, 10, and 27 December; 27 March; 8, 11 (twice), 12 (twice), 16, 18, and 20 April; 19, 28, and 30 July; 13–14, 19, 20, 24, and 25 August; 4, 5, 7, 15, and 19 September; 5, 13, and 16 October; and 15 November. Around 76% of these events lasted for no longer than 5 h, consistent with the findings by Lei and Wang (2014) that the majority of the exceptional dust storms in Arizona during 2003–2012 lasted 2–5 h mainly due to meso- or small-scale weather systems (e.g., thunderstorms, convections along dry lines, and gusty winds caused by high pressure systems). Hourly PM10 during these high dust periods ranged from 57 to $8540\,\mu\mathrm{g\,m^{-3}}$, with the PM2.5 / PM10 ratio between ~ 0.07 and ~ 0.2, and PM2.5 was highly correlated with PM10 during these peri-
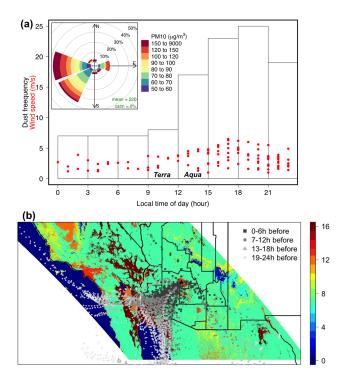
Figure 5. (a) Frequency of identified dust storms in Phoenix in 2007 as a function of the time of occurrence. Hourly mean wind speed (∼ half of the hourly maximum, with correlation coefficient of ∼ 0.93) during these dust storms is shown in red dots, and the inset panel shows the frequencies of PM10 within various concentration intervals by wind direction during these dust storms. **(b)** Hourly HYSPLIT endpoints colored by four time intervals, overlaid on a 500 m MODIS land cover type image. The MODIS land cover types mentioned in the text and their corresponding numbers are barren or sparsely vegetated: 16; urban and built-up: 13; open shrublands: 7; cropland: 12; and cropland/native vegetation: 14 (source: https://lpdaac.usgs.gov/dataset_discovery/modis/modis_products_table/mcd12q1).

Figure 6. (a) NAQFC 12 km CMAQ modeled 24 h mean surface PM2.5 on 11 May 2014, with the AirNow (circles) and IMPROVE (triangles) observations overlaid. **(b)** CMAQ modeled dust contributions (%) to the total PM2.5 on this day. Locations of AirNow (circles) and IMPROVE (triangles) are shown. Observed (black) and modeled (red) surface PM2.5 in **(c)** Maricopa and **(d)** Pima counties on this day, at AQS (solid lines) and IMPROVE (dashed lines) sites.

ods ($r > 0.9$). In April–May 2007, the Pacific Dust Experiment (PACDEX) was carried out to study dust emission and transport from Asia (Stith et al., 2009). The University of Iowa STEM chemical transport model tracer calculations (http://data.eol.ucar.edu/codiac/dss/id=96.013) estimated dust to be ∼ 2 µg m⁻³ on average (and not exceeding 10 µg m⁻³ during transport events) at ∼ 5.3 km altitude in Arizona during this period, which can serve as the upper limit of extra-regional dust impacts on the surface PM concentrations. During our identified dust events, PM10 concentrations were much higher than this magnitude and therefore were mainly due to the impact from local dust emissions.

The identified high dust periods were validated using the hourly AQS trace gas observations. Figure S5 includes the scatterplots of AQS CO and NO$_x$ over the PM10 measurements at the Phoenix JLG AQS site. Two distinct slopes are shown in both scatterplots, representing the times mainly affected by anthropogenic/biomass burning sources and dust.
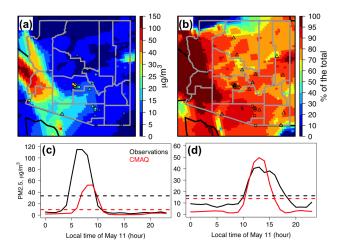
PM10 values during most of the identified dust events fall into the slope ends in these scatterplots. Using the PM2.5 / PM10 ratio as an additional constraint (as suggested in Tong et al., 2012; Lei and Wang, 2014) in the second step of selection excluded some less strong events interfered by anthropogenic/biomass burning emission sources but possibly also some real dust events. After the second step of selection, higher-than-median CO or NO$_x$ values were observed at only ∼ 10 % of the identified dust times. In addition, AQS qualifier codes provide useful information for interpreting the event types, e.g., the IJ and RJ flags (https://aqs.epa.gov/aqsweb/codes/data/QualifierCodes.html) inform that 19–20 July was a high wind event.

Independent IMPROVE and satellite observations can also assist in validating these identified dust events. IMPROVE observations were only available on ∼ 29 % of these identified dusty days (7 and 10 December; 12 and 18 April; 13, 19, and 25 August; 15 September), and they were more likely to be able to indicate exceptionally strong and long-lasting events due to the 24 h sampling duration. Tong et al. (2012) reported two strong dust storm events at the PHOE1 IMPROVE site (∼ 12 April; ∼ 20 July) using total PM concentrations and its speciation, both of which were also captured by our method. In addition, ∼ 48 % of the days impacted by strong blowing dust were possibly captured by MODIS (i.e., dust events occurred between 09:00 and 15:00 LT: 10 December; 27 March; 11, 12, 16, 18, and 20 April; 19 and 30 July; 7 and 15 September; 15 November). To further demonstrate the advantages of using frequently sampled observations for capturing dust events, we plotted the time of occur-

Table 2. Evaluation of NAQFC CMAQ PM2.5 predictions during a recent dust storm event on 11 May 2014.

County in Arizona	Site type	No. of sites	Observed PM2.5*	Modeled PM2.5*	Correlation coefficient (observed vs. modeled)
Maricopa	AirNow	8	23.7 ± 37.6	9.6 ± 16.2	0.7
	IMPROVE	2	33.7	9.5	–
Pima	AirNow	5	16.7 ± 12.6	10.9 ± 15.8	0.9
	IMPROVE	2	16.3	13.8	–

* Units in $\mu g\,m^{-3}$; mean $\pm$ standard deviation during this 24 h period shown for the AirNow results.
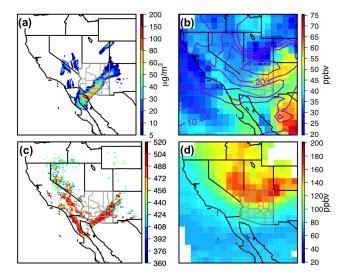

Figure 7. (a) CMAQ modeled dust contributions to PM2.5 and **(b)** RAQMS modeled surface ozone at 11:00 mountain standard time on 11 May 2014. The purple contour lines in **(b)** indicate RAQMS relative humidity (%) at the upper troposphere ($\sim 300\,hPa$). **(c)** and **(d)** indicate, respectively, the AIRS daytime (early afternoon overpass time) dust score and ozone concentrations at 300 hPa. Following the criteria at http://disc.sci.gsfc.nasa.gov/nrt/data-holdings/airs-nrt-products, the dust score values below 360 were rejected.

rence of these AQS-/AZMET-based dust periods in Phoenix for this year (Fig. 5a). Dust events occurred more frequently during Aqua overpass times than during the Terra overpasses, consistent with the findings from Fig. 2. Most of these dust events occurred between 15:00 and 21:00 LT, when winds were stronger (also in Fig. 5a) and the soil was drier (derived by looking at NAM soil moisture at the top soil layer in recent years, not shown), rather than at MODIS overpass times from late morning to early afternoon times. A similar long-term diurnal variability of dust event occurrence has been found in Utah based on analyzing the weather code (Hahnenberger and Nicoll, 2012). Therefore, current polar orbiting satellites are unable to observe all dust events, and the hourly sampling frequency of the future geostationary satellites can help better capture dust events together with the surface monitoring network. Such conclusions were also drawn

by Schepanski et al. (2012) for the African dust source regions.

We classified PM mass by wind direction observed at the Phoenix AZMET site, which indicates the dominant westerly/southwesterly winds at the Phoenix high dust times. Furthermore, based on the NARR meteorology, HYSPLIT air mass trajectories were originated from 500 m above the ground level (a.g.l.) of Phoenix at the identified dust periods to locate the origins of Phoenix dust episodes and indicate the regional transport patterns. The endpoints of these HYSPLIT backtrajectories are overlaid on the MODIS land classification map (Fig. 5b), showing that most of the transported dust particles were at the shrublands or deserts (primarily Sonoran, also Chihuahuan) 0–12 h before arriving in urban Phoenix areas below $\sim 900\,hPa$. This is consistent with the finding from Figs. 3 and S1, in which barren and sparsely vegetated open shrubland are the major contributors to the dust producing areas in 2007.

3.4 Case study of a recent strong dust event accompanied by a stratospheric ozone intrusion

Multiple satellites identified a recent dust event (10–11 May 2014) in the western US: as described by NOAA's HMS text product (http://www.ssd.noaa.gov/PS/FIRE/DATA/SMOKE/2014/2014E111659.html; http://www.ssd.noaa.gov/PS/FIRE/DATA/SMOKE/2014/2014E120143.html), dust was originated in southern California. It swept across northern Baja California and Arizona, and then entered New Mexico after a cold-frontal boundary and impacted Texas, Oklahoma and Kansas. We evaluated the current NAQFC PM2.5 (a standard NAQFC air quality modeling product) forecasting skill during this event and assessed the impact of dust emission on the regional air quality based on model sensitivity analysis. The NAQFC 12 km CMAQ base simulation produced 24 h mean PM2.5 of over $50\,\mu g\,m^{-3}$ in western Arizona and $> 15\,\mu g\,m^{-3}$ in southwestern Arizona on 11 May 2014 (Fig. 6a). A sensitivity analysis using the base and no-dust simulations indicates that over $50\,\mu g\,m^{-3}$ of hourly PM2.5 during this event were contributed from dust emissions in populated urban regions in Arizona (such as Phoenix in the Maricopa county and Tucson in the Pima

county) and, on average, dust contributed to $>70\%$ of the total PM2.5 in most Arizona grid cells (Fig. 6b).

The modeled PM2.5 was evaluated mainly for the Maricopa and Pima counties in Arizona where both IMPROVE and AirNow observations were available during this event. Time series of observed and modeled PM2.5 are shown in Fig. 6c and d. AirNow observations indicate daily maxima to be over $100\,\mu g\,m^{-3}$ in Maricopa (at $\sim 08{:}00\,LT$) and over $50\,\mu g\,m^{-3}$ in Pima (at $\sim 14{:}00\,LT$), with PM2.5 / PM10 ratios at the dust times below 0.2 (not shown). Both the model and observations show significant temporal variability (standard deviations), indicating the advantages of the AirNow data for capturing the extremely high PM concentrations during the dust events. The model was fairly well correlated with the observations (with median/high correlation coefficients of 0.7–0.9; Table 2). CMAQ underpredicted the daily maxima in Maricopa by a factor of ~ 2 with a 2 h lag, while it slightly overpredicted them in Pima with the right timing. PM was measured at more AirNow sites than at IMPROVE sites in both counties on this day. The observed 24 h mean concentration at the AirNow sites was lower than at the IMPROVE sites in Maricopa, but those in Pima were close. This can be mainly due to the different sampling areas that AirNow and IMPROVE networks cover. The model underpredicted the 24 h mean values in both counties, with more significant negative biases in Maricopa than in Pima.

This dust event was accompanied by a stratospheric ozone intrusion, as shown from a RAQMS model simulation that assimilated ozone columns from the Ozone Monitoring Instrument and ozone profiles from the Microwave Limb Sounder, as well as the AIRS satellite products (Figs. 7, S6). Descending dry air containing rich ozone enhanced the surface ozone concentrations in eastern Arizona and New Mexico at late morning and early afternoon times, when dust was strongly impacting the same locations. Observed surface ozone at the Petrified Forest National Park in eastern Arizona (AQS/AirNow site no. 040170119) at this time exceeded 65 ppbv. However, the current NAQFC CMAQ modeling system is unable to capture the exceptionally high ozone during stratospheric intrusion episodes, as the CMAQ lateral boundary conditions were downscaled from the monthly mean GEOS-Chem simulation in 2006 and no upper boundary conditions were used.

4 Conclusions and suggestions

We developed dust records in Arizona for 2005–2013 using multiple observation data sets, including the MODIS level 2 deep blue aerosol product and in situ measurements at the surface AQS and IMPROVE sites in Phoenix. Both satellite and surface aerosol observations were anticorrelated with three drought indicators (i.e., NDVI, soil moisture, and PDSI). Dust events were stronger and more frequent in the afternoon times than in the morning due to stronger winds

and drier soil; in addition, the Sonoran and Chihuahuan deserts were important dust source regions during the identified dust events in Phoenix. These findings suggest a potential for use of satellite soil moisture and land products to interpret and predict dust activity. We also emphasized the importance of using hourly observations for the better representation of dust events, and we expect that the hourly geostationary satellite observations will in future complement the current surface PM and meteorological observations, especially considering their broader spatial coverage. Continued development of products from the polar-orbiting satellites is also important in that they can provide higher-spatial-resolution observations from each swath due to their lower orbit level. Future efforts should also be devoted to better characterizing and attributing the observed dust, by integrating additional satellite measurements (such as ammonia as shown in Ginoux et al., 2012b) and in situ measurements of trace gases and aerosol compositions.

In a case study, we evaluated the capability of the current NAQFC CMAQ modeling system to capture the magnitude of aerosol concentrations and their temporal variability during a recent dust event. Sensitivity simulations from this modeling system assessed the impact of this dust event on western US air quality, and showed that dust contributed to $>70\%$ of the total PM2.5 in Arizona, on average. Satellite weather and land products are currently being integrated into dust emission modeling for future improvement of NAQFC's PM forecasting skill. Finally, we showed that this recent dust event was accompanied by a stratospheric ozone intrusion, and we emphasized the importance of representing both PM and ozone well under such conditions.

The Supplement related to this article is available online at doi:10.5194/acp-15-12595-2015-supplement.

References

Alley, W. M.: The Palmer drought severity index: Limitation and Assumptions, J. Climate Appl. Meteor., 23, 1100–1109, 1984.

Appel, K. W., Pouliot, G. A., Simon, H., Sarwar, G., Pye, H. O. T., Napelenok, S. L., Akhtar, F., and Roselle, S. J.: Evaluation of dust and trace metal estimates from the Community Multiscale Air Quality (CMAQ) model version 5.0, Geosci. Model Dev., 6, 883–899, doi:10.5194/gmd-6-883-2013, 2013.

Baddock, M. C., Bullard, J. E., and Bryant, R. G.: Dust source identification using MODIS: a comparison of techniques applied to the Lake Eyre Basin, Australia, Remote Sens. Environ., 113, 1511–1528, 2009.

Barrett, S. R. H., Yim, S. H. L., Gilmore, C. K., Murray, L. T., Kuhn, S. R., Tai, A. P. K., Yantosca, R. M., Byun, D. W., Ngan, F., Li, X., Levy, J., Ashok, A., Koo, J., Wong, H. M., Dessens, O., Balasubramanian, S., Fleming, G. G., Wollersheim, C., Malina, R., Pearlson, M. N., Arunachalam, S., Binkowski, F. S., Leibensperger, E. M., Jacob, D. J., Hileman, J. I., and Waitz, I. A.: Public health, climate and economic impacts of desulfurizing jet fuel, Environ. Sci. Technol., 46, 4275–4282, doi:10.1021/es203325a, 2012.

Bian, J., Gettelman, A., Chen, H., and Pan, L. L.: Validation of satellite ozone profile retrievals using Beijing ozonesonde data, J. Geophys. Res., 112, D06305, doi:10.1029/2006JD007502, 2007.

Brahney, J., Ballantyne, A. P., Sievers, C., and Neff, J. C.: Increasing Ca^{2+} deposition in the western US: the role of mineral aerosols, Aeol. Res., 10, 77–87, 2013.

Brown, M. E., Pinzon, J. E., Didan, K., Morisette, J. T., and Tucker, C. J.: Evaluation of the consistency of long-term NDVI time series derived from AVHRR, SPOT-Vegetation, SeaWiFS, MODIS and Landsat ETM+, IEEE Trans. Geosci. Remote Sens., 44, 1787–1793, 2006.

Byun, D. and Schere, K. L.: Review of the Governing Equations, Computational Algorithms, and Other Components of the Models-3 Community Multiscale Air Quality (CMAQ) Modeling System, Appl. Mech. Rev., 59, 51–77, 2006.

Carslaw, K. S., Boucher, O., Spracklen, D. V., Mann, G. W., Rae, J. G. L., Woodward, S., and Kulmala, M.: A review of natural aerosol interactions and feedbacks within the Earth system, Atmos. Chem. Phys., 10, 1701–1737, doi:10.5194/acp-10-1701-2010, 2010.

Chai, T., Kim, H.-C., Lee, P., Tong, D., Pan, L., Tang, Y., Huang, J., McQueen, J., Tsidulko, M., and Stajner, I.: Evaluation of the United States National Air Quality Forecast Capability experimental real-time predictions in 2010 using Air Quality System ozone and NO2 measurements, Geosci. Model Dev., 6, 1831–1850, doi:10.5194/gmd-6-1831-2013, 2013.

Chen, H. and Grassian, V. H.: Iron Dissolution of Dust Source Materials during Simulated Acidic Processing: The Effect of Sulfuric, Acetic, and Oxalic Acids, Environ. Sci. Technol., 47, 10312–10321, doi:10.1021/es401285s, 2013.

Chin, Mian, Diehl, T., Ginoux, P., and Malm, W.: Intercontinental transport of pollution and dust aerosols: implications for regional air quality, Atmos. Chem. Phys., 7, 5501–5517, doi:10.5194/acp-7-5501-2007, 2007.

Creamean, J. M., Suski, K. J., Rosenfeld, D., Cazorla, A., DeMott, P. J., Sullivan, R. C., White, A. B., Ralph, F. M., Minnis, P., Comstock, J. M., Tomlinson, J. M., and Prather, K. A.: Dust and bio-logical aerosols from the Sahara and Asia influence precipitation in the western US, Science, 339, 1572–1578, 2013.

Creamean, J. M., Ault, A. P., White, A. B., Neiman, P. J., Ralph, F. M., Minnis, P., and Prather, K. A.: Impact of interannual variations in sources of insoluble aerosol species on orographic precipitation over California's central Sierra Nevada, Atmos. Chem. Phys., 15, 6535–6548, doi:10.5194/acp-15-6535-2015, 2015.

Csavina, J., Field, J., Félix, O., Corral-Avitia, A.Y., Sáez, A. E., and Betterton, E. A.: Effect of wind speed and relative humidity on atmospheric dust concentrations in semi-arid climates, Sci. Total Environ., 487, 82–90, doi:10.1016/j.scitotenv.2014.03.138, 2014.

Dai, A., Trenberth, K. E., and Qian, T.: A global data set of Palmer Drought Severity Index for 1870–2002: Relationship with soil moisture and effects of surface warming, J. Hydrometeorol., 5, 1117–1130, 2004.

Dentener, F. J., Carmichael, G. R., Zhang, Y., Lelieveld, J., and Crutzen, P. J.: Role of mineral aerosol as a reactive surface in the global troposphere, J. Geophys. Res., 101, 22869–22889, doi:10.1029/96JD01818, 1996.

Draxler, R. R. and Hess, G. D.: An overview of the HYSPLIT_4 modeling system for trajectories, dispersion, and deposition, Aust. Meteorol. Mag., 47, 295–308, 1998.

Draxler, R. R. and Rolph, G. D.: HYSPLIT (HYbrid Single-Particle Lagrangian Integrated Trajectory) Model access via NOAA ARL READY Website, NOAA Air Resources Laboratory, Silver Spring, MD, http://ready.arl.noaa.gov/HYSPLIT.php, last access: June, 2015.

Draxler, R. R., Ginoux, P., and Stein, A. F.: An empirically derived emission algorithm for windblown dust, J. Geophys. Res., 115, D16212, doi:10.1029/2009JD013167, 2010.

Dunlea, E. J., DeCarlo, P. F., Aiken, A. C., Kimmel, J. R., Peltier, R. E., Weber, R. J., Tomlinson, J., Collins, D. R., Shinozuka, Y., McNaughton, C. S., Howell, S. G., Clarke, A. D., Emmons, L. K., Apel, E. C., Pfister, G. G., van Donkelaar, A., Martin, R. V., Millet, D. B., Heald, C. L., and Jimenez, J. L.: Evolution of Asian aerosols during transpacific transport in INTEX-B, Atmos. Chem. Phys., 9, 7257–7287, doi:10.5194/acp-9-7257-2009, 2009.

Eguchi, K., Uno, I., Yumimoto, K., Takemura, T., Shimizu, A., Sugimoto, N., and Liu, Z.: Trans-pacific dust transport: integrated analysis of NASA/CALIPSO and a global aerosol transport model, Atmos. Chem. Phys., 9, 3137–3145, doi:10.5194/acp-9-3137-2009, 2009.

Fairlie, T. D., Jacob, D. J., and Park, R. J.: The impact of transpacific transport of mineral dust in the United States, Atmos. Environ., 41, 1251–1266, 2007.

Fairlie, T. D., Jacob, D. J., Dibb, J. E., Alexander, B., Avery, M. A., van Donkelaar, A., and Zhang, L.: Impact of mineral dust on nitrate, sulfate, and ozone in transpacific Asian pollution plumes, Atmos. Chem. Phys., 10, 3999–4012, doi:10.5194/acp-10-3999-2010, 2010.

Fischer, E. V., Hsu, N. C., Jaffe, D. A., Jeong, M.-J., and Gong, J. C.: A decade of dust: Asian dust and springtime aerosol load in the U.S. Pacific Northwest, Geophys. Res. Lett., 36, L03821, doi:10.1029/2008GL036467, 2009.

Friedl, M. A., Sulla-Menashe, D., Tan, B., Schneider, A., Ramankutty, N., Sibley, A., and Huang, X.: MODIS Collection 5

global land cover: Algorithm refinements and characterization of new datasets, Remote Sens. Environ., 114, 168–182, 2010.

Gassó, S., Grassian, V. H., and Miller, R. L.: Interactions between Mineral Dust, Climate and Ocean Ecosystems, Elements, 6, 247–253, doi:10.2113/gselements.6.4.247, 2010.

Ginoux, P. and Torres, O.: Empirical TOMS index for dust aerosol: Applications to model validation and source characterization, J. Geophys. Res., 108, 4534, doi:10.1029/2003JD003470, 2003.

Ginoux, P., Chin, M., Tegen, I., Prospero, J. M., Holben, B., Dubovik, O., and Lin, S.-J.: Sources and distributions of dust aerosols simulated with the GOCART model, J. Geophys. Res., 106, 20255–20274, 2001.

Ginoux, P., Prospero, J. M., Torres, O., and Chin, M.: Long-term simulation of global dust distribution with the GOCART model: Correlation with North Atlantic Oscillation, Environ. Modell. Softw., 19, 113–128, doi:10.1016/S1364-8152(03)00114-2, 2004.

Ginoux, P., Garbuzov, D., and Hsu, H. C.: Identification of anthropogenic and natural dust sources using Moderate Resolution Imaging Spectroradiometer (MODIS) Deep Blue level 2 data, J. Geophys. Res., 115, D05204, doi:10.1029/2009JD012398, 2010.

Ginoux, P., Prospero, J. M., Gill, T. E., Hsu, N. C., and Zhao, M.: Global-scale attribution of anthropogenic and natural dust sources and their emission rates based on MODIS deep blue aerosol products, Rev. Geophys., 50, RG3005, doi:10.1029/2012RG000388, 2012a.

Ginoux, P., Prospero, J. M., Gill, T. E., Hsu, N. C., and Zhao, M.: Global-scale attribution of anthropogenic and natural dust sources and their emission rates based on MODIS deep blue aerosol products, Rev. Geophys., 50, RG3005, doi:10.1029/2012RG000388, 2012b.

Goudie, A. S.: Desert dust and human health disorders, Environ. Int., 63, 101–113, doi:10.1016/j.envint.2013.10.011, 2013.

Grassian, V. H.: Heterogeneous Uptake and Reaction of Nitrogen Oxides and Volatile Organic Compounds on the Surface of Atmospheric Particles Including Oxide, Carbonate, Soot and Mineral Dust: Implications for the Chemical Balance of the Troposphere, Int. Rev. Phys. Chem., 20, 467–548, doi:10.1080/01442350110051968, 2001.

Hahnenberger, M. and Nicoll, K.: Meteorological characteristics of dust storm events in the eastern Great Basin of Utah, USA, Atmos. Environ., 60, 601–612, doi:10.1016/j.atmosenv.2012.06.029, 2012.

Hedin, L. O. and Likens, G. E.: Atmospheric Dust And Acid Rain, Sci. Am., 275, 88–92, 1996.

Hsu, N. C., Jeong, M.-J., Bettenhausen, C., Sayer, A. M., Hansell, R., Seftor, C. S., Huang, J., and Tsay, S.-C.: Enhanced Deep Blue aerosol retrieval algorithm: The second generation, J. Geophys. Res. Atmos., 118, 9296–9315, doi:10.1002/jgrd.50712, 2013.

Janjic, Z., Black, T., Pyle, M., Chuang, H., Rogers, E., and DiMego, G.: An Evolutionary Approach to Nonhydrostatic Modeling, Symposium on the 50th Aniversary of Operational Numerical Weather Prediction, College Park, MD, Amer. Meteor. Soc, available at: http://www.wrf-model.org/wrfadmin/publications/Chuang_Janjic_NWP50yearsfinalshort.pdf, 2004.

Janjic, Z. I.: A nonhydrostatic model based on a new approach, Meteorol. Atmos. Phys., 82, 271–285, doi:10.1007/s00703-001-0587-6, 2003.

Ji, L. and Peters, A. J.: Assessing vegetation response to drought in the northern Great Plains using vegetation and drought indices, Remote Sens. Environ., 87, 85–98, 2003.

Karl, T. R. and Koss, W. J.: Regional and National Monthly, Seasonal, and Annual Temperature Weighted by Area, 1895–1983, Historical Climatology Series 4–3, National Climatic Data Center, Asheville, NC, 38 pp., 1984.

Karnieli, A., Agam, N., Pinker, R. T., Anderson, M., Imhoff, M. L., and Gutman, G. G.: Use of NDVI and land surface temperature for drought assessment: Merits and limitations, J. Climate, 23, 618–633, doi:10.1175/2009JCLI2900.1, 2010.

Kavouras, I. G., Etyemezian, V., Xu, J., DuBois, D. W., Green, M., and Pitchford, M.: Assessment of the local windblown component of dust in the western United States, J. Geophys. Res., 112, D08211, doi:10.1029/2006JD007832, 2007.

Kim, D., Chin, M., Bian, H., Tan, Q., Brown, M. E., Zheng, T., You, R., Diehl, T., Ginoux, P., and Kucsera, T.: The effect of the dynamic surface bareness to dust source function, emission, and distribution, J. Geophys. Res., 118, 1–16, doi:10.1029/2012JD017907, 2013.

Kim, H. and Choi, M.: Impact of soil moisture on dust outbreaks in East Asia: Using satellite and assimilation data, Geophys. Res. Lett., 42, 2789–2796. doi:10.1002/2015GL063325, 2015.

Kim, Y., Ou, M.-L., Ryoo, S.-B., Chun, Y., Lee, E.-H., and Hong, S.: Soil moisture retrieved from microwave satellite data and its relationship with the Asian dust (Hwangsa) frequency in East Asia during the period from 2003 to 2010, Asia-Pac. J. Atmos. Sci., 49, 527–534, 2013.

Langford, A. O., Senff, C. J., Alvarez II, R. J., Brioude, J., Cooper, O. R., Holloway, J. S., Lin, M. Y., Marchbanks, R. D., Pierce, R. B., Sandberg, S. P., Weickmann, A. M., and Williams, E. J.: An overview of the 2013 Las Vegas Ozone Study (LVOS): Impact of stratospheric intrusions and long-range transport on surface air quality, Atmos. Environ, 109, 305–322, doi:10.1016/j.atmosenv.2014.08.040, 2014.

Lee, J. A. and Gill, T. E.: Multiple causes of wind erosion in the dust bowl, Aeol. Res., 19, 15–36, doi:10.1016/j.aeolia.2015.09.002, 2015.

Lei, H. and Wang, J. X. L.: Observed characteristics of dust storm events over the western United States using meteorological, satellite, and air quality measurements, Atmos. Chem. Phys., 14, 7847–7857, doi:10.5194/acp-14-7847-2014, 2014.

Li, X. L. and Zhang, H. S.: Soil moisture effects on sand saltation and dust emission observed over Horqin Sandy Land area in China, J. Meteorol. Res., 28, 445–452, 2014.

Lin, M., Fiore, A. M., Cooper, O. R., Horowitz, L. W., Langford, A. O., Levy II, H., Johnson, B. J., Naik, V., Oltmans, S. J., and Senf, C. J.f: Springtime high surface ozone events over the western United States: Quantifying the role of stratospheric intrusions, J. Geophys. Res., 117, D00V22, doi:10.1029/2012JD018151, 2012.

Liu, J., Mauzerall, D. L., and Horowitz, L. W.: Evaluating intercontinental transport of fine aerosols: (2) Global health impact, Atmos. Environ., 43, 4339–4347, 2009a.

Liu, J., Mauzerall, D. L., Horowitz, L. W., Ginoux, P., and Fiore, A. M.: Evaluating Inter-continental transport of fine aerosols: (1) Methodology, global aerosol distribution and optical depth, Atmos. Environ., 43, 4327–4338, doi:10.1016/j.atmosenv.2009.03.054, 2009b.

Liu, X., Yin, Z.-Y., Zhang, X., and Yang, X.: Analyses of the spring dust storm frequency of northern China in relation to antecedent and concurrent wind, precipitation, vegetation, and soil moisture conditions, J. Geophys. Res., 109, D16210, doi:10.1029/2004JD004615, 2004.

Mahler, A.-B., Thome, K., Yin, D., and Sprigg, W. A.: Dust transport model validation using satellite and ground-based methods in the southwestern United States, Proc. SPIE 6299, Remote Sensing of Aerosol and Chemical Gases, Model Simulation/Assimilation, and Applications to Air Quality, 62990L, doi:10.1117/12.679868, 2006.

Mahowald, N. M., Ballantine, J. A., Feddema, J., and Ramankutty, N.: Global trends in visibility: implications for dust sources, Atmos. Chem. Phys., 7, 3309–3339, doi:10.5194/acp-7-3309-2007, 2007.

Malm, W. C., Schichtel, B. A., Pitchford, M. L., Ashbaugh, L. L., and Eldred, R. A.: Spatial and monthly trends in speciated fine particle concentration in the United States, J. Geophys. Res., 109, D03306, doi:10.1029/2003JD003739, 2004.

Melillo, J. M., Richmond, T. C., and Yohe, G. W. (Eds.): Climate Change Impacts in the United States: The Third National Climate Assessment, US Global Change Research Program, 841 pp., doi:10.7930/J0Z31WJ2, 2014.

Mesingera, F., DiMego, G., Kalnay, E., Mitchell, K., Shafran, P. C., Ebisuzaki, W., Jovic, D., Woollen, J., Rogers, E., Berbery, E. H., Ek, M. B., Fan, Y., Grumbine, R., Higgins, W., Li, H., Lin, Y., Manikin, G., Parrish, D., and Shi, W.: North American Regional Reanalysis, B. Am. Meteor. Soc., 87, 343–360, doi:10.1175/BAMS-87-3-343, 2006.

McQueen, J., Huang, J., Shafran, P., Rogers, E., Pondeca, M., DiMego, G., and Stajner, I.: Evaluation of NCEP Atmospheric Models for Driving Air Quality Prediction, 27th Conference on Weather Analysis and Forecasting, Chicago, IL, available at: https://ams.confex.com/ams/27WAF23NWP/webprogram/Paper273598.html (last access: October 2015), 2015a.

McQueen, J., Lee, P., Huang, J., Huang, H.-C., Shafran, P., Rogers, E., Pondeca, M., DiMego, G., and Stajner, I.: NWS NWP models and their Potential Impact for Air Quality Prediction, 7th International workshop on air quality research, College Park, MD, available at: http://www.arl.noaa.gov/documents/IWAQFR/Presentations2015/S4_McQueen_IWAQFR_2015.pdf (last access: October 2015), 2015b.

Miller, R. L., Perlwitz, J.P., and Tegen, I.: Feedback upon dust emission by dust radiative forcing through the planetary boundary layer, J. Geophys. Res., 109, D24209, doi:10.1029/2004JD004912, 2004a.

Miller, R. L., Tegen, I., and Perlwitz, J. P.: Surface radiative forcing by soil dust aerosols and the hydrologic cycle, J. Geophys. Res., 109, D04203, doi:10.1029/2003JD004085, 2004b.

Morain, S. A., Budge, A. M., and Sprigg, W. A.: Modeling atmospheric dust for respiratory health alerts, Atlanta, GA, available at: https://ams.confex.com/ams/90annual/techprogram/paper_165772.htm, 2010.

Nordstrom, K. F. and Hotta, S.: Wind erosion from cropland in the USA:A review of problems, solutions and prospects, Geoderma, 12, 157–167, doi:10.1016/j.geoderma.2003.11.012, 2004.

Painter, T. H., Barrett, A. P., Landry, C. C., Neff, J. C., Cassidy, M. P., Lawrence, C. R., McBride, K. E., and Farmer, G. L.: Impact of disturbed desert soils on duration of mountain snow cover, Geophys. Res. Lett., 34, L12502, doi:10.1029/2007GL030284, 2007.

Palmer, W. C: Meteorological Drought. Res. Paper No. 45, 58pp., Dept. of Commerce, Washington, D.C., p. 58, 1965.

Pan, L. and Randel, B.: Dynamical Variability of Ozone near the Tropopause from AIRS Data, AIRS science tem meeting, Pasadena, CA, available at: http://airs.jpl.nasa.gov/documents/science_team_meeting_archive/2006_09/slides/Pan_AIRS06Fallf.pdf (last access: October 2015), 2006.

Pan, L., Tong, D. Q., Lee, P., Kim, H., and Chai, T.: Assessment of NO_x and O_3 forecasting performances in the U.S. National Air Quality Forecasting Capability before and after the 2012 major emissions updates, Atmos. Environ., 95, 610–619, doi:10.1016/j.atmosenv.2014.06.020, 2014.

Pan, L. L., Bowman, K. P., Shapiro, M., Randel, W. J., Gao, R. S., Campos, T., Davis, C., Schauffler, S., Ridley, B. A., Wei, J. C., and Barnet, C.: Chemical behavior of the tropopause observed during the Stratosphere-Troposphere Analyses of Regional Transport experiment, J. Geophys. Res., 112, D18110, doi:10.1029/2007JD008645, 2007.

Panikkath, R., Jumper, C. A., and Mulkey, Z.: Multilobar lung infiltrates after exposure to dust storm: the Haboob Lung Syndrome, Am J. Med., 126, 5–7, 2013.

Pierce, R. B., Schaack, T., Al-Saadi, J. A., Fairlie, T. D., Kittaka, C., Lingenfelser, G., Natarajan, M., Olson, J., Soja, A., Zapotocny, T., Lenzen, A., Stobie, J., Johnson, D., Avery, M. A., Sachse, G. W., Thompson, A., Cohen, R., Dibb, J. E., Crawford, J., Rault, D., Martin, R., Szykman, J., and Fishman, J.: Chemical data assimilation estimates of continental US ozone and nitrogen budgets during the Intercontinental Chemical Transport Experiment–North America, J. Geophys. Res., 112, D12S21, doi:10.1029/2006JD007722, 2007.

Prospero, J. M., Ginoux, P., Torres, O., Nicholson, S. E., and Gill, T. E.: Environmental characterization of global sources of atmospheric soil dust identified with the Nimbus 7 Total Ozone Mapping Spectrometer (TOMS) absorbing aerosol product, Rev. Geophys., 40, 1002, doi:10.1029/2000RG000095, 2002.

Raman, A. and Arellano Jr., F. A.: Modeling and Data Analysis of 2011 Phoenix Dust Storm, 93rd AMS annual meeting, Austin, TX, available at: https://ams.confex.com/ams/93Annual/webprogram/Paper214743.html (last access: October 2015), 2013.

Ravi, S., D'Odorico, P., Breshears, D. D., Field, J. P., Goudie, A. S., Huxman, T. E., Li, J., Okin, G. S., Swap, R. J., Thomas, A. D., Van Pelt, S., Whicker, J. J., and Zobeck, T. M.: Aeolian processes and the biosphere, Rev. Geophys., 49, RG3001, doi:10.1029/2010RG000328, 2011.

Reddy, P. and Pierce, B: Current State of Practice in Identifying and Forecasting Stratospheric Intrusion Events, Air Quality Applied Sciences Team 3rd Meeting, Madison, WI, available at: http://acmg.seas.harvard.edu/aqast/meetings/2012_jun/AM_20120614/1000_AQASTJune2012Reddy.pdf (last access: October 2015), 2012.

Reynolds, R., Belnap, J., Reheis, M., Lamothe, P., and Luiszer, F.: Aeolian dust in Colorado Plateau soils: Nutrient inputs and recent change in source, P. Natl. Acad. Sci. USA, 98, 7123–7127, doi:10.1073/pnas.121094298, 2001.

Reynolds, R., Neff, J., Reheis, M., and Lamothe, P.: Atmospheric dust in modern soil on aeolian sandstone, Colorado Plateau (USA): Variation with landscape position and contribution to potential plant nutrients, Geoderma, 130, 108–123, doi:10.1016/j.geoderma.2005.01.012, 2006.

Sayer, A. M., Hsu, N. C., Bettenhausen, C., and Jeong, M.-J.: Validation and uncertainty estimates for MODIS Collection 6 "Deep Blue" aerosol data, J. Geophys. Res. Atmos., 118, 7864–7872, doi:10.1002/jgrd.50600, 2013.

Scheftic, W., Zeng, X., Broxton, P., and Brunke, M.: Intercomparison of Seven NDVI Products over the United States and Mexico, Remote Sens., 6, 1057–1084, 2014.

Schepanski, K., Tegen, I., and Macke, A.: Comparison of satellite based observations of Saharan dust source areas, Remote Sens. Environ., 123, 90–97, doi:10.1016/j.rse.2012.03.019, 2012.

Shao, Y., Klose, M., and Wyrwoll, K.-H.: Recent global dust trend and connections to climate forcing, J. Geophys. Res. Atmos., 118, 11107–11118, doi:10.1002/jgrd.50836, 2013.

Shi, Y., Zhang, J., Reid, J. S., Hyer, E. J., and Hsu, N. C.: Critical evaluation of the MODIS Deep Blue aerosol optical depth product for data assimilation over North Africa, Atmos. Meas. Tech., 6, 949–969, doi:10.5194/amt-6-949-2013, 2013.

Sprigg, W. A., Nickovic, S., Galgiani, J. N., Pejanovic, G., Petkovic, S., Vujadinovic, M., Vukovic, A., Dacic, M., DiBiase, S., Prasad, A., and El-Askary, H.: Regional dust storm modeling for health services: The case of valley fever, Aeol. Res., 14, 53–73, doi:10.1016/j.aeolia.2014.03.001, 2014.

Stein, A., Draxler, R., Rolph, G., Stunder, B., Cohen, M., and Ngan, F.: NOAA's HYSPLIT atmospheric transport and dispersion modeling system, B. Amer. Meteor. Soc., doi:10.1175/BAMS-D-14-00110.1, in press, 2015.

Stith, J. L., Ramanathan, V., Cooper, W. A., Roberts, G. C., DeMott, P. J., Carmichael, G., Hatch, C. D., Adhikary, B., Twohy, C. H., Rogers, D. C., Baumgardner, D., Prenni, A. J., Campos, T., Gao, R., Anderson, J., and Feng, Y.: An overview of aircraft observations from the Pacific Dust Experiment campaign, J. Geophys. Res., 114, D05207, doi:10.1029/2008JD010924, 2009.

Tanaka, T. Y. and Chiba, M.: A numerical study of the contributions of dust source regions to the global dust budget, Global Planet Change, 52, 88–104, 2006.

Tong, D. Q., Dan, M., Wang, T., and Lee, P.: Long-term dust climatology in the western United States reconstructed from routine aerosol ground monitoring, Atmos. Chem. Phys., 12, 5189–5205, doi:10.5194/acp-12-5189-2012, 2012.

Tong, D. Q., Bowker, G. E., He, S., Byun, D. W., Mathur, R., and Gillette, D. A.: Development of a windblown dust emission model FENGSHA: description and initial application in the United States, , in review, 2015.

Torres, O., Bhartia, P. K., Herman, J. R., Syniuk, A., Ginoux, P., and Holben, B.: A long term record of aerosol optical depth from TOMS observations D and comparison to AERONET measurements, J. Atm. Sci., 59, 398–413, 2002.

Tucker, C. J. and Choudhury, B. J.: Satellite remote sensing of drought conditions, Remote Sens. Environ., 23, 23243–251, 1987.

Underwood, G. M., Song, C. H., Phadnis, M., Carmichael, G. R., and Grassian, V. H.: Heterogeneous reactions of NO_2 and HNO_3 on oxides and mineral dust: A combined laboratory and modeling study, J. Geophys. Res., 106, 18055–18066, doi:10.1029/2000JD900552, 2001.

Uno, I., Eguchi, K., Yumimoto, K., Takemura, T., Shimizu, A., Uematsu, M., Liu, Z., Wang, Z., Hara, Y., and Sugimoto, N.: Asian dust transported one full circuit around the globe, Nat. Geosci., 2, 557–560, doi:10.1038/ngeo583, 2009.

Van Curen, R. A. and Cahill, T. A.: Asian aerosols in North America: Frequency and concentration of fine dust, J. Geophys. Res., 107, 4804, doi:10.1029/2002JD002204, 2002.

Vukovic, A., Vujadinovic, M., Pejanovic, G., Andric, J., Kumjian, M. R., Djurdjevic, V., Dacic, M., Prasad, A. K., El-Askary, H. M., Paris, B. C., Petkovic, S., Nickovic, S., and Sprigg, W. A.: Numerical simulation of "an American haboob", Atmos. Chem. Phys., 14, 3211–3230, doi:10.5194/acp-14-3211-2014, 2014.

Wan, Z., Wang, P., and Li, X.: Using MODIS land surface temperature and normalized difference vegetation index products for monitoring drought in the Southern Great Plains, USA, Int. J. Remote Sens., 25, 61–72, 2004.

Wang, D., Morton, D., Masek, J., Wu, A., Nagol, J., Xiong, X., Levy, R., Vermote, E., and Wolfe, R.: Impact of sensor degradation on the MODIS NDVI time series, Remote Sens. Environ., 119, 55–61, 2012.

Warner, J. X., McCourt Comer, M., Barnet, C. D., McMillan, W. W., Wolf, W., Maddy, E., and Sachse, G.: A comparison of satellite tropospheric carbon monoxide measurements from AIRS and MOPITT during INTEX-A, J. Geophys. Res., 112, D12S17, doi:10.1029/2006JD007925, 2007.

Yasunari, T. J. and Yamazaki, K.: Impacts of Asian dust storm associated with the stratosphere-to-troposphere transport in the spring of 2001 and 2002 on dust and tritium variations in Mount Wrangell ice core, Alaska, Atmos. Environ., 43, 2582–2590, doi:10.1016/j.atmosenv.2009.02.025, 2009.

Yasunari, T. J., Shiraiwa, T., Kanamori, S., Fujii, Y., Igarashi, M., Yamazaki, K., Benson, C. S., and Hondoh, T.: Intraannual variations in atmospheric dust and tritium in the North Pacific region detected from an ice core from Mount Wrangell, Alaska, J. Geophys. Res., 112, D10208, doi:10.1029/2006JD008121, 2007.

Yin, D., Nickovic, S., and Sprigg, W. A.: The impact of using differet land cover data on wind-blown desert dust modeling results in the southwestern United States, Atmos. Environ., 41, 2214–2224, doi:10.1016/j.atmosenv.2006.10.061, 2007.

Yu, H., Chin, M., Yuan, T., Bian, H., Remer, L. A., Prospero, J. M., Omar, A., Winker, D., Yang, Y., Zhang, Y., Zhang, Z., and Zhao, C.: The fertilizing role of African dust in the Amazon rainforest: A first multiyear assessment based on data from Cloud-Aerosol Lidar and Infrared Pathfinder Satellite Observations, Geophys. Res. Lett., 42, 1984–1991, doi:10.1002/2015GL063040, 2015.

Zender, C. S., Newman, D., and Torres, O.: Spatial heterogeneity in aeolian erodibility: Uniform, topographic, geomorphic, and hydrologic hypotheses, J. Geophys. Res., 108, 4543, doi:10.1029/2002JD003039, 2003.

Zender, C. S., Miller, R. L. L., and Tegen, I.: Quantifying mineral dust mass budgets: Terminology, constraints, and current estimates, Eos Trans. AGU, 85, 509–512, doi:10.1029/2004EO480002, 2004.

Zhao, C., Liu, X., and Leung, L. R.: Impact of the Desert dust on the summer monsoon system over Southwestern North America, Atmos. Chem. Phys., 12, 3717–3731, doi:10.5194/acp-12-3717-2012, 2012.

Zhu, C., Wang, B., and Qian, W.: Why do dust storms decrease in northern China concurrently with the recent global warming?, Geophys. Res. Lett., 35, L18702, doi:10.1029/2008GL034886, 2008.